

Article

Determination of Fumonisin B₁ by Aptamer-Based Fluorescence Resonance Energy Transfer

Xinyue Zhao [†], Jiale Gao [†], Yuzhu Song , Jinyang Zhang  and Qin Qin Han ^{*}

Faculty of Life Science and Technology, Kunming University of Science and Technology, Kunming 650500, China

^{*} Correspondence: hanqq@kust.edu.cn; Tel.: +86-(0871)-65939528[†] These authors contributed equally to this work.

Abstract: Fumonisin FB is produced by *Fusarium moniliforme* Sheld, of which FB₁ is the most common and the most toxic. The establishment of a rapid detection method is an important means to prevent and control FB₁ pollution. A highly sensitive fluorescent sensor based on an aptamer for the rapid detection of fumonisin B₁ (FB₁) in corn was established. In this study, 5-carboxyfluorescein (FAM) was labeled on the aptamer of FB₁ (F10). F10 was adsorbed on the surface of graphene oxide (GO) by π - π stacking. The FAM fluorescence signal could be quenched by fluorescence resonance energy transfer between fluorescent molecules and graphene oxide (GO). In the presence of FB₁, the binding efficiency of the aptamer to GO was reduced. Therefore, the content of FB₁ in corn samples was determined by fluorescence measurements of mixed FAM-labeled F10, GO and corn samples. This method had a good linear relationship in an FB₁ concentration range of 0–3000 ng/mL. The equation was $y = 0.2576x + 10.98$, $R^2 = 0.9936$. The limit of detection was 14.42 ng/mL, and the limit of quantification was 43.70 ng/mL. The recovery of a spiked standard in the corn sample was 89.13–102.08%, and the time of detection was 30 min.

Keywords: fumonisin B₁; aptamer; fluorescence resonance energy transfer; graphene oxide; corn flour



Citation: Zhao, X.; Gao, J.; Song, Y.; Zhang, J.; Han, Q. Determination of Fumonisin B₁ by Aptamer-Based Fluorescence Resonance Energy Transfer. *Sensors* **2022**, *22*, 8598. <https://doi.org/10.3390/s22228598>

Academic Editors: Simone Morais, Álvaro Miguel Carneiro Torrinha and Iria Bravo

Received: 7 October 2022

Accepted: 2 November 2022

Published: 8 November 2022

Publisher's Note: MDPI stays neutral with regard to jurisdictional claims in published maps and institutional affiliations.



Copyright: © 2022 by the authors. Licensee MDPI, Basel, Switzerland. This article is an open access article distributed under the terms and conditions of the Creative Commons Attribution (CC BY) license (<https://creativecommons.org/licenses/by/4.0/>).

1. Introduction

Fumonisin FB, produced by *Fusarium moniliforme* Sheld, is an important mycotoxin. Several mycotoxin types exist, namely fumonisin A₁ (FA₁), fumonisin A₂ (FA₂), fumonisin B₁ (FB₁), fumonisin B₂ (FB₂), fumonisin B₃ (FB₃), and others, of which FB₁ is the most common and the most toxic [1]. It has been classified as a class 2B carcinogen by the International Agency for Research on Cancer (IARC) [2,3]. China's National Food Safety guidelines do not specify a limit for FB₁ in food, but the European Union and the U.S. Food and Drug Administration have set the upper limit for FB₁ in feed as 200–2000 µg/kg and 3000–4000 µg/kg, respectively [4]. Corn is the crop most polluted by FB₁, which has also been detected in wheat and soybeans. As corn is the most common crop in animal feed, pollution can lead to serious adverse events in animals eating contaminated feed [2]. The mechanism of FB₁ toxicity is based on the inhibition of sphingolipid biosynthesis, which is an important cellular event, and the inhibition of sphingolipid biosynthesis can lead to organ failure [5,6]. Existing studies have demonstrated that a variety of diseases in mammals can be caused by FB₁, such as equine white matter encephalomalacia [7], porcine pulmonary edema [8], mouse liver tumor development [9], and acute kidney poisoning in goats [10]. FB₁ can also cause serious adverse events in chickens and other types of poultry, such as sudden weight loss, shrinkage of organs (e.g., spleen), acute myocarditis, liver injury, and increased mortality [11–13]. Therefore, the establishment of a method for the detection of possible FB₁ residues in food samples is of great importance for food safety monitoring.

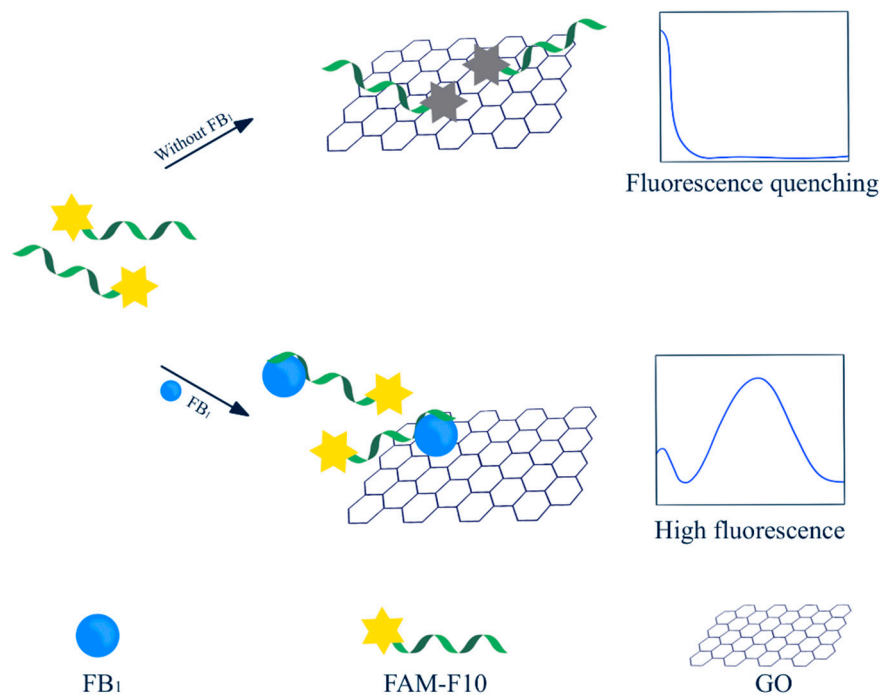
The enzyme-linked immunosorbent assay (ELISA) is a standard analytical technique used to monitor mycotoxin pollution in food and animal feed. Shu et al. established a

one-step competitive ELISA to quickly and efficiently detect FB₁ in grain samples. The limit of detection (LOD) of the colorimetric ELISA was 0.35 ng/mL, and there was a good linear relationship between 0.93 and 7.73 ng/mL. The LOD of the chemiluminescent ELISA was 0.12 ng/mL, and there was a good linear relationship between 0.29 and 2.68 ng/mL [14]. Although ELISA has the advantages of high sensitivity and exceptional convenience, it also has some disadvantages, such as relatively poor stability and high antibody costs. Molecularly imprinted polymers (MIPs) have been used in various analyses and sensors, and they have demonstrated great potential in the replacement of antibodies used in ELISA [15,16]. Munawar et al. proposed a competitive method based on molecularly imprinted polymer nanoparticles (MINAs), in which FB₁ is fixed on a solid carrier for the preparation of nano MIPs, and the LOD was 1.9 pM in the concentration range of 10 pM–10 nM [5]. Qian et al. used a Max column combined with high-performance liquid chromatography–tandem mass spectrometry to detect FB₁ in dairy products. Upon the addition of FB₁ in a concentration range of 0.1–5 µg/L to milk, the authors revealed that the recovery was 76.4–92.3%. The LODs of FB₁, FB₂, and their hydrolytic metabolites were 0.03, 0.03, and 0.1 µg/L, respectively [17]. However, the above technologies involve high costs, and require significant human and material resources, which need to be analyzed by experienced researchers. The electrochemical method has relatively high sensitivity, low LOD, and strong specificity in target recognition. Zheng et al. established an electrochemical detection sensor. The sensor showed a good linear relationship at an FB₁ concentration range of 1×10^{-11} – 1×10^{-4} g/mL, and the LOD was 10 pg/mL [18]. Based on the antigen antibody reaction and color development characteristics of colloidal gold, the immunochromatography assay (ICA), with colloidal gold as the medium, has been widely used in the field of rapid detection. Ren et al. developed a colloidal gold test strip for FB₁ detection by ICA with an LOD of 2.5 ng/mL and used it for the rapid detection of FB₁ in corn [19]. Because antibodies are expensive and other materials are in short supply, the research and development of test strips requires significant human and other resources. The above-mentioned methods have several advantages, namely low LOD and reliability; however, the cost is high, and on-site rapid detection is challenging. Therefore, it is necessary to introduce low-cost raw materials with strong affinity, and specificity, and an aptamer is a good choice.

Aptamers are single-stranded DNA or RNA that specifically bind to a target (small molecule or protein) with high affinity and selectivity [20]. Aptamers have the ability to amplify the signal of the sensor, and signal amplification is a key component of ultrasensitive analysis for the detection of trace amounts of analytical targets, such as various biologically significant macro and small molecules, disease biomarkers, toxins, bacterial pathogens or viruses, and environmental contamination [21]. Aptamers have also played a significant role in advancing cancer treatment, with alpha-PCNA (proliferating cell nuclear antigen) aptamers as therapeutic aptamers and adriamycin as a chemotherapeutic drug instrument delivered to tumor cells for precision treatment [22]. Aptamer biosensing systems have significantly improved the quantitative detection of molecular biomarkers of various harmful diseases, such as ovarian cancer. Farzin et al. developed a silver-nanoparticle-modified, kainamine-oxime-modified, polyacrylonitrile-nanofiber-based build for the sensitive detection of CA125 with an LOD of 0.0042 U/mL [23]. In the field of food safety detection, Talari et al. developed an optical probe nanosensor based on multiwalled carbon nanotubes and reduced graphene quantum dots for the specific detection of the organophosphorus pesticide diazinon with a detection limit of 0.4 nM (0.14 µg/L) [24].

The specific FB₁ aptamer F10 with high affinity was successfully selected by the systematic evolution of ligands by exponential enrichment (SELEX) [25]. In this study, a fluorescent sensor was designed for the specific detection of FB₁. F10 was labeled with a fluorescent molecule (FAM), and the fluorescence of F10 could be quenched by GO. GO is a type of nanomaterial with higher quenching efficiency. Compared with other quenchers, it can maintain the stability of biomolecules on its surface and prevent enzyme digestion [26]. As shown in Scheme 1, in the absence of FB₁, π - π stacking promoted FB₁-specific aptamer

F10 adsorption on the surface of GO. The fluorescence resonance energy transfer (FRET) interaction between fluorescent molecules and GO resulted in the quenching of the FAM fluorescent signal. The method had a good linear relationship in the FB₁ concentration range of 0–3000 ng/mL, and the LOD was 14.42 ng/mL. The method was used to detect FB₁ in corn flour samples, and recovery was high, consistent with the ELISA results.



Scheme 1. Schematic diagram of the FRET method for detecting FB₁ based on the aptamer.

2. Materials and Methods

2.1. Reagents and Apparatuses

FB₁ was purchased from Binzhi Biotechnology (Shanghai, China). Ochratoxin A (OTA) was purchased from Xiheng Biotechnology (Shanghai, China). Zearalenone (ZEN) was purchased from Fubo Biotechnology (Beijing, China). Aflatoxin B₁, aflatoxin G₁, and aflatoxin G₂ were purchased from Sigma-Aldrich Corporation (St. Louis, MO, USA). NaCl, KI, Cl, and Na₂HPO₄·12H₂O were purchased from Tianjin No. 3 Chemical Reagent Factory (Tianjin, China). CH₃OH was purchased from Corus Chemical Co., Ltd. (Shanghai, China). KH₂PO₄ was purchased from Shanghai Aladdin Biochemical Technology Co., Ltd. (Shanghai, China). GO dispersion was purchased from Nanjing Xianfeng Nanomaterials Technology Co., Ltd. (Nanjing, China). All reagents used in this study were of analytical grade. Deionized water (18.2 MX) was used in buffer preparation, and 0.01 M phosphate-buffered saline (pH = 7.4, PBS) was used for fluorescence measurements. The corn flour samples were obtained from local markets. The aptamer used in this study was synthesized by Tsingke Biological Technology (Beijing, China). The sequence of the F10 was 5'-FAM-CGA TCT GGA TAT TAT TTT TGA TAC CCC TTT GGG GAG ACA T-3'. An Agilent G9800A spectrofluorometer (Agilent Technologies, Santa Clara, CA, USA) was used for obtaining the spectra. A Thermo BIOMATE 3S microplate reader (USA) was used for reading the absorbance of the ELISA.

2.2. Specificity of the Fluorescent Aptasensor for FB₁ Detection

In order to verify the specificity of the fluorescence sensor, under the above optimized conditions, several other common mycotoxins that coexist with FB₁ in corn grains (AFB₁, AFG₁, AFG₂, ZEN, and OTA) were used as negative controls, and PBS was used as the blank control for the specificity study. FAM-F10 was added to the tubes to give a final

concentration of 50 nM in a 3 mL system. AFB₁, AFG₁, AFG₂, ZEN, OTA, FB₁, and a toxin mixture were added to the tubes to give a final concentration of 200 ng/mL for each toxin. The final volume of each tube was adjusted to 3 mL with PBS (pH = 7.4). The mixed system was incubated in a constant-temperature shaker at 37 °C and 60 rpm for 10 min. GO, at a concentration of 46 µg/mL, was added to the system after 10 min of incubation, and the system was thoroughly mixed. The excitation wavelength was set to 497 nm, and the fluorescence value was measured at 520 nm.

2.3. Sensitivity of the Fluorescent Chemosensor for FB₁ Detection

To further investigate the sensitivity of the fluorescence sensor and the linear relationship between toxin concentration and fluorescence values, different concentrations of FB₁ were added to the system containing 50 nM FAM-F10. A concentration gradient of FB₁ was established as follows: 0, 10, 15, 40, 80, 100, and 200 ng/mL. The final volume was made up to 3 mL by fixing with PBS. The mixed system was incubated in a constant-temperature shaker at 37 °C and 60 rpm for 10 min. GO, at a concentration of 46 µg/mL, was added to the system, and the system was thoroughly mixed. The excitation wavelength was set to 497 nm, and the fluorescence value was measured at 520 nm.

2.4. Analysis of FB₁ in the Corn Flour Samples

Firstly, 10 g of the two corn powders was dissolved in 50 mL of methanol, and the solutions were thoroughly mixed and then centrifuged at 4000 rpm for 20 min at 4 °C. Next, the supernatant was collected and filtered through a 0.22 µm filter membrane and diluted three times with double-distilled water, 10 times each. The two samples, designated as 1 and 2, were stored at 4 °C. Standard FB₁ solution was added into each tube, so that the final concentrations were 0, 20, 80, and 200 ng/mL, and PBS was used to adjust the volume to 3 mL. A final concentration of 50 nM of the aptamer FAM-F10 was added to each tube. The mixed system was incubated in a constant-temperature shaker at 37 °C and 60 rpm for 10 min. GO was added to the system at a concentration of 46 µg/mL, and the system was mixed to measure the fluorescence value. The parameters of the fluorometer were set to an excitation wavelength of 497 nm, and the fluorescence was recorded at 520 nm. An FB₁ ELISA kit was used to validate the results of the spiked recovery experiments for both samples. To analyze the data, the above experiments were repeated three times independently.

3. Results and Discussion

3.1. Principle of Fluorescent Sensors

Modification of the FAM fluorescent tag at one end of the aptamer makes it highly fluorescent, and GO is an excellent fluorescent quenching agent. When the target FB₁ does not exist in the system, the addition of FAM-F10 coupling can adsorb on the GO surface by p-p stacking, and the FRET between the fluorescent molecule and GO rapidly quenches the fluorescence and measures a low fluorescence value. When the target FB₁ exists in the system, the FAM-F10 coupling binds to the target, thus greatly reducing the binding efficiency of GO and FAM and measuring a high fluorescence value. As shown in Figure 1A, when FAM-F10, GO, and FB₁ were simultaneously added to the system, the fluorescence significantly increased. Therefore, it was demonstrated that the specific binding between FAM-F10 and FB₁ could significantly reduce the binding efficiency of GO and FAM and the quenching efficiency of GO, thereby rendering the fluorescence unable to be completely quenched.

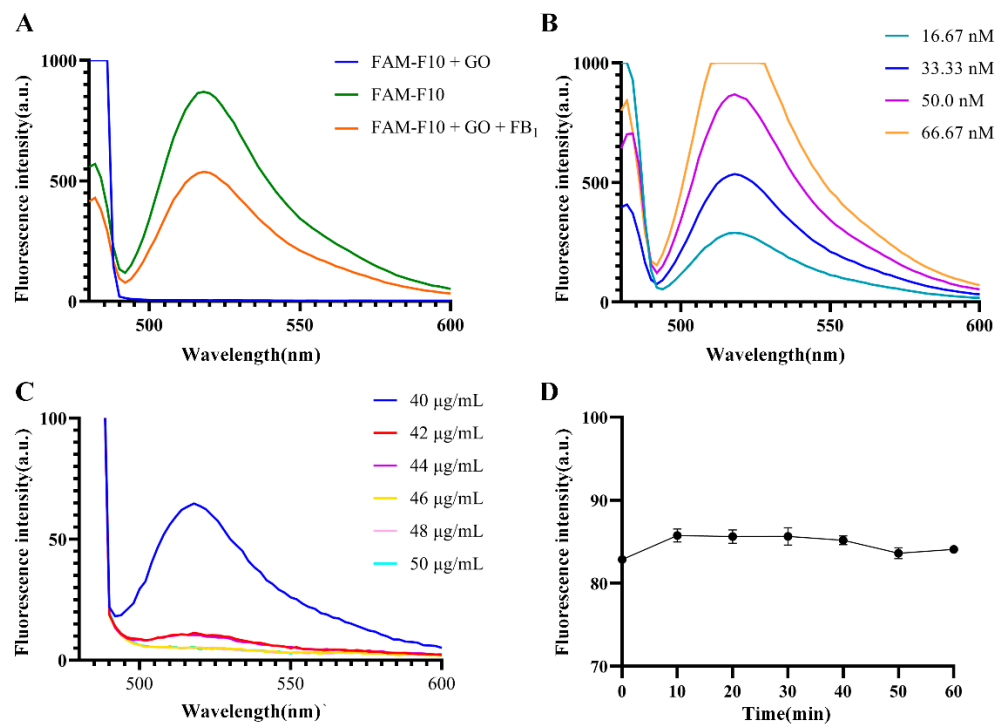


Figure 1. Optimization of experimental conditions. (A) Relationship between fluorescence intensity and wavelength in the presence of FB₁. (B) Optimization of the FAM-F10 concentration. (C) Optimization of the GO concentration. (D) Optimization of the incubation time.

3.2. Optimization of the FAM-F10 Conjugate Concentration

Excessive FAM–aptamer conjugation can cause the fluorescence value to exceed the range that the fluorometer can detect. In order to make the measured fluorescence value within the detectable range, different concentrations of FAM-F10 were used for fluorescence detection. The aptamer FAM-F10 was added to the tubes to prepare final concentrations of 16.67, 33.33, 50.00, and 66.67 nM, and the volume was adjusted to 3 mL with PBS (pH 7.4). The excitation wavelength of the fluorescence spectrometer was set to 497 nm, and the fluorescence value was recorded at 520 nm. GO was added to the system to completely quench the fluorescence. As shown in Figure 1B, when the concentration of FAM-F10 was 50 nM, the fluorescence measurement at 520 nm was at the highest value that was within the detection range of the instrument. Therefore, 50 nM was selected as the optimal concentration of FAM-F10.

3.3. Optimization of GO Concentration

GO can burst the fluorescence of FAM fluorescent groups. In this study, as GO is able to completely burst the fluorescence of FAM, the presence of the target FB₁ in the system could return the fluorescence value to achieve the detection of the minimum concentration of FB₁ in the system, so the GO concentration was optimized. Under the optimal concentration of FAM-F10, GO was added to the tubes to prepare final concentrations of 40, 42, 44, 46, 48, and 50 μg/mL, and the volume was adjusted to 3 mL with PBS (pH = 7.4). The excitation wavelength of the fluorescence spectrometer was set to 497 nm, and the fluorescence value was recorded at 520 nm. High GO concentrations led to complete fluorescence quenching, while low GO concentrations led to incomplete quenching, resulting in the high fluorescence of the system. As shown in Figure 1C, GO, at a concentration of 46 μg/mL, was sufficient to completely quench the fluorescence. Therefore, this concentration was used as the optimal concentration of GO for subsequent detection assays.

3.4. Optimization of the Incubation Time

To make sure that FAM-F10 and FB₁ were completely combined and the fluorescence value was stabilized, it was necessary to optimize the incubation time. Under the optimal concentration of FAM-F10, FB₁ was added into the tubes to prepare a final concentration of 300 ng/mL, and then mixed for 1 min, followed by incubation in a constant-temperature shaking table at 37 °C and 60 rpm. The incubation time was set to 10, 20, 30, 40, 50, and 60 min. The excitation wavelength of the fluorescence spectrometer was set to 497 nm, and the fluorescence value was recorded at 520 nm. When the fluorescence values were stable, the target was completely bound to the aptamer. The optimization results are shown in Figure 1D. The fluorescence intensity gradually increased within 10 min and then stabilized. Therefore, the incubation time of FAM-F10 and FB₁ was set to 10 min.

3.5. Specificity of the Fluorescent Aptasensor for FB₁ Detection

Although the aptamer could specifically bind to the target, the established fluorescent sensor still required specific verification. Other mycotoxins coexisting with FB₁ were used as controls to verify the selectivity of the fluorescent sensor. In this study, AFB₁, AFG₁, AFG₂, ZEN, OTA, and all toxin mixtures, including FB₁, were used as controls. The results are shown in Figure 2. The fluorescence measurements at 520 nm in the blank control group and the negative control groups of AFB₁, AFG₁, AFG₂, ZEN, and OTA were at their lowest levels. The quenching efficiency of GO to FAM was the strongest, and the quenching efficiency was not reduced after the addition of toxins. In contrast, the fluorescence measurements at 520 nm in the toxin mixture and FB₁ standard solution groups were significantly different from those of the other groups; the fluorescence values were significantly higher than those of the other groups. These results demonstrated that the sensor had strong specificity and selectivity.

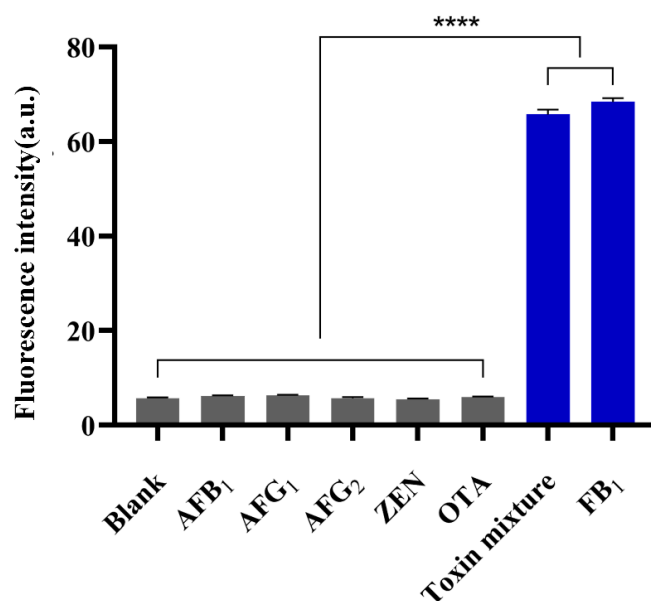


Figure 2. Specificity of the sensor for the detection of FB₁. (Toxin mixture included AFB₁, AFG₁, ZEN, OTA and FB₁, **** $p < 0.001$).

3.6. Sensitivity of the Fluorescent Aptasensor for FB₁ Detection

According to the principles of sensor detection, there should be a positive correlation between the concentration of FB₁ in the system and the fluorescence value measured at 520 nm. With the gradual increase in the FB₁ concentration in the system, the quenching efficiency of GO to FAM gradually decreased, and the fluorescence value measured at 520 nm accordingly increased. As shown in Figure 3A, by setting the gradient of FB₁ and analyzing the fluorescence values of FB₁ at different concentrations, a standard curve

with the FB₁ concentration as the abscissa and the fluorescence intensity as the ordinate could be obtained, in which $R^2 = 0.9936$ and the equation of the standard curve was $y = 0.2576x + 10.98$. Figure 3B shows that when the concentration of FB₁ was in the range of 0–3000 ng/mL, the fluorescence intensity had an obvious linear relationship with the FB₁ concentration. The LOD and LOQ were calculated using the following data. The formula for the LOD was $3.3 \times \sigma/S$, where σ is the standard deviation of the test value of the blank group, and S is the slope of the standard curve. Similarly, the formula for the LOQ was $10 \times \sigma/S$. Under optimal conditions, the LOD of the method was 14.42 ng/mL, and the LOQ was 43.70 ng/mL.

A fluorescent sensor based on fluorescently labeled aptamer FAM-F10 and GO for FB₁ detection was established. There are many methods to detect FB₁, such as antibody-based flowmetric immunoassays with detection limits of 0.025 and 0.097 ng/mL in corn and feed, respectively [27]. In contrast with the reported antibody-based approach, a FAM fluorescent group was modified at the 5' end of the FB₁-specific binding aptamer F10 to provide fluorescence properties, and a GO with fluorescence bursting properties was subtly introduced. The aptamer used in this experiment has the significant advantages of low cost and good batch-to-batch consistency compared with the antibody. Compared with other methods using fluorescence burst [28], one of the advantages of this method is that it combines the fluorescent-group-labeled FAM with the aptamer, which ensures the stability of fluorescence and simplifies the experimental process by eliminating the step of incubating the aptamer with other materials [29]. Compared with LC-MC, the sample pre-treatment in this study is simpler and easier for actual sample detection [30]. Compared with the ELNOA method [31], the FRET method requires less time and fewer steps to measure FB₁, which greatly saves time and costs. In terms of LOD, the detection limit of ELNOA is lower than that of FRET, but both methods can meet the detection requirements of the EU and FAD. The FRET method enables rapid on-site detection (POCT) due to the popularity of portable fluorometers.

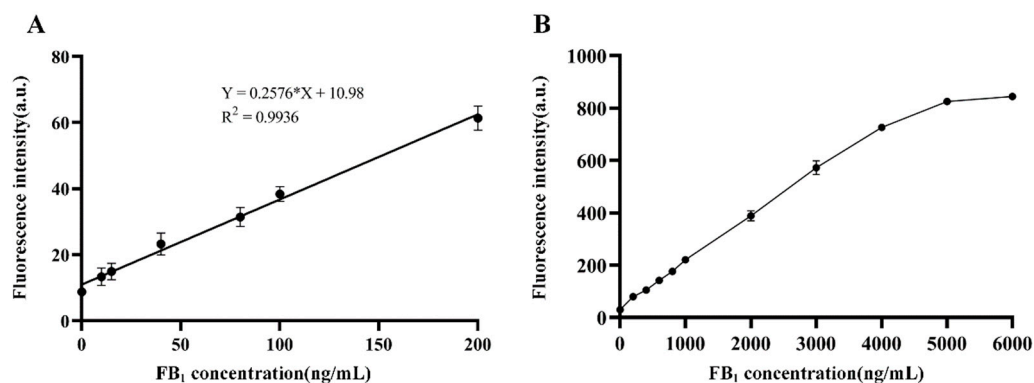


Figure 3. Sensitivity of the fluorescent aptasensor for FB₁ detection. (A) Linear relationship between the fluorescence and the FB₁ concentration (0, 10, 15, 40, 80, 100, and 200 ng/mL). (B) Detection range of the fluorescent aptasensor for FB₁ detection.

3.7. Detection of FB₁ in Corn Flour Samples

To verify the detection accuracy of the fluorescence sensor using actual samples, two types of corn flour were pretreated, and the FB₁ standard solution was added to the two samples to prepare FB₁ concentrations of 0, 20, 80, and 200 ng/mL. The fluorescence sensor and ELISA generated in this study were used for standard addition and recovery experiments. As shown in Table 1, the recovery of corn flour sample 1 measured by this method was 89.13–98.66%, and the recovery detected by the ELISA was 98.35–100%. The recovery of corn flour sample 2 was 90.7–102.08%, and the recovery by the ELISA was 97.73–99.42%. Thus, it was confirmed that the results obtained by the constructed sensor were highly consistent with the detection results of the ELISA, which proved the accuracy

of the detection results. Therefore, it was verified that the proposed sensor can be used to detect the content of FB₁ in actual samples.

Table 1. Comparison of the detection results of FB₁ in corn samples between FRET and the ELISA.

| Sample | Addition Amount (ng/mL) | Detection Value (ng/mL) | Recovery (%) | Detection Value (ELISA) (ng/mL) | Recovery (%) |
|----------|-------------------------|-------------------------|--------------|---------------------------------|--------------|
| Sample 1 | 20 | 19.73 ± 5.46 | 98.66 | 19.74 ± 0.09 | 98.35 |
| | 80 | 71.25 ± 5.82 | 89.13 | 79.90 ± 0.08 | 100.00 |
| | 200 | 195.01 ± 2.19 | 96.61 | 197.41 ± 0.09 | 98.71 |
| Sample 2 | 20 | 18.25 ± 6.17 | 91.23 | 19.55 ± 0.44 | 97.73 |
| | 80 | 72.56 ± 2.58 | 90.7 | 79.53 ± 0.39 | 99.42 |
| | 200 | 204.15 ± 11.51 | 102.08 | 195.46 ± 0.44 | 97.73 |

4. Conclusions

In this study, the FRET method was established by fluorescently labeling FAM on an FB₁-specific nucleic acid aptamer and using the ability of GO to burst the fluorescence to establish a fluorescent sensor. By optimizing the GO concentration, under the premise that GO is able to burst the fluorescence of FAM, as long as a trace amount of FB₁ is present in the system, FB₁ can enter into specific binding with F10, so that GO cannot burst the fluorescence of FAM, and its fluorescence value is significantly rebounded compared with the fluorescence value at complete burst. The method is characterized by high sensitivity and wide detection range, with good linearity in the concentration range of 0–3000 ng/mL. LOD was as low as 14.42 ng/mL, and the spiked recovery experiments confirmed that the method could efficiently detect FB₁ in maize samples with recoveries of 89.13–102.08%. Based on the excellent properties of the aptamer, the established fluorescent sensor provides a new idea for the design of other target detection methods with a wide range of applications.

Author Contributions: Conceptualization, Q.H.; methodology, Q.H.; validation, Q.H., X.Z. and J.G.; formal analysis, Q.H., X.Z. and J.G.; investigation, Q.H., Y.S. and J.Z.; data curation, Q.H.; writing—original draft preparation, X.Z. and J.G.; writing—review and editing, Q.H. and J.G.; visualization, X.Z. and J.G.; supervision, Q.H.; project administration, Q.H.; funding acquisition, Q.H. All authors have read and agreed to the published version of the manuscript.

Funding: This research was funded by the National Natural Science Foundation of China (NSFC Grant No. 32160601) and Basic Research Projects of Yunnan Province (No. 202001AT070033).

Acknowledgments: We thank Kunming University of Science and Technology for providing all the facilities for this research and the Natural Science Foundation of China (NSFC grant No. 32160601) and Basic research projects of Yunnan Province (No. 202001AT070033) for financial support.

Conflicts of Interest: The authors declare no conflict of interest.

References

1. Wang, X.; Wu, Q.; Wan, D.; Liu, Q.; Chen, D.; Liu, Z.; Martínez-Larrañaga, M.R.; Martínez, M.A.; Anadón, A.; Yuan, Z. Fumonisin: Oxidative stress-mediated toxicity and metabolism in vivo and in vitro. *Arch. Toxicol.* **2015**, *90*, 81–101. [[CrossRef](#)] [[PubMed](#)]
2. Acuña-Gutiérrez, C.; Schock, S.; Jiménez, V.M.; Müller, J. Detecting fumonisin B₁ in black beans (*Phaseolus vulgaris* L.) by near-infrared spectroscopy (NIRS). *Food Control* **2021**, *130*, 108335. [[CrossRef](#)]
3. Alsulami, T.; Nath, N.; Flemming, R.; Wang, H.; Zhou, W.; Yu, J.-H. Development of a novel homogeneous immunoassay using the engineered luminescent enzyme NanoLuc for the quantification of the mycotoxin fumonisin B₁. *Biosens. Bioelectron.* **2020**, *177*, 112939. [[CrossRef](#)] [[PubMed](#)]
4. Huang, X.; Huang, X.; Xie, J.; Li, X.; Huang, Z. Rapid simultaneous detection of fumonisin B₁ and deoxynivalenol in grain by immunochromatographic test strip. *Anal. Biochem.* **2020**, *606*, 113878. [[CrossRef](#)] [[PubMed](#)]
5. Munawar, H.; Smolinska-Kempisty, K.; Cruz, A.G.; Canfarotta, F.; Piletska, E.; Karim, K.; Piletsky, S.A. Molecularly imprinted polymer nanoparticle-based assay (MINA): Application for fumonisin B₁ determination. *Analyst* **2018**, *143*, 3481–3488. [[CrossRef](#)]

6. Yu, S.; Jia, B.; Liu, N.; Yu, D.; Zhang, S.; Wu, A. Fumonisin B1 triggers carcinogenesis via HDAC/PI3K/Akt signalling pathway in human esophageal epithelial cells. *Sci. Total Environ.* **2021**, *787*, 147405. [[CrossRef](#)]
7. Marasas, W.F.; Kellerman, T.S.; Pienaar, J.G.; Naudé, T.W. Leukoencephalomalacia: A mycotoxicosis of Equidae caused by *Fusarium moniliforme* Sheldon. *Onderstepoort J. Vet. Res.* **1976**, *43*, 113–122.
8. Kriek, N.P.; Kellerman, T.S.; Marasas, W.F. A comparative study of the toxicity of *Fusarium verticillioides* (=F. *moniliforme*) to horses, primates, pigs, sheep and rats. *Onderstepoort J. Vet. Res.* **1981**, *48*, 129–131.
9. Gelderblom, W.C.A.; Snyman, S.D. Mutagenicity of potentially carcinogenic mycotoxins produced by *Fusarium moniliforme*. *Mycotoxin Res.* **1991**, *7*, 46–52.
10. Edrington, T.S.; Kamps-Holtzapfel, C.A.; Harvey, R.B.; Kubena, L.F.; Elissalde, M.H.; Rottinghaus, G.E. Acute hepatic and renal toxicity in lambs dosed with fumonisin-containing culture material. *J. Anim. Sci.* **1995**, *73*, 508–515. [[CrossRef](#)]
11. Marijanovic, D.R.; Holt, P.; Norred, W.P.; Bacon, C.W.; Voss, K.A.; Stancel, P.C.; Ragland, W.L. Immunosuppressive Effects of *Fusarium moniliforme* Corn Cultures in Chickens. *Poult. Sci.* **1991**, *70*, 1895–1901. [[CrossRef](#)] [[PubMed](#)]
12. Espada, Y.; Ruiz de Gopegui, R.; Cuadradas, C.; Cabañes, F.J. Fumonisin mycotoxicosis in broilers: Plasma proteins and co-agulation modifications. *Avian Dis.* **1997**, *41*, 73–79. [[PubMed](#)]
13. Javed, T.; Bennett, G.A.; Richard, J.L.; Dombrink-Kurtzman, M.A.; Buck, W.B. Mortality in broiler chicks on feed amended with *Fusarium proliferatum* culture material or with purified fumonisin B1 and moniliformin. *Mycopathologia* **1993**, *123*, 171–184. [[CrossRef](#)] [[PubMed](#)]
14. Shu, M.; Xu, Y.; Liu, X.; Li, Y.; He, Q.; Tu, Z.; Fu, J.; Gee, S.J.; Hammock, B.D. Anti-idiotypic nanobody-alkaline phosphatase fusion proteins: Development of a one-step competitive enzyme immunoassay for fumonisin B₁ detection in cereal. *Anal. Chim. Acta* **2016**, *924*, 53–59. [[CrossRef](#)]
15. Canfarotta, F.; Poma, A.; Guerreiro, A.; Piletsky, S. Solid-phase synthesis of molecularly imprinted nanoparticles. *Nat. Protoc.* **2016**, *11*, 443–455. [[CrossRef](#)]
16. Tang, Y.; Gao, J.; Liu, X.; Gao, X.; Ma, T.; Lu, X.; Li, J. Ultrasensitive detection of clenbuterol by a covalent imprinted polymer as a biomimetic antibody. *Food Chem.* **2017**, *228*, 62–69. [[CrossRef](#)]
17. Qian, M.R.; Wu, L.Q.; Hu, Z.; Fei, L.; Rui, L.; Zhi-Min, C.; Fang, L.Z. Determination of Fumonisin B-1, B-2 and Their Hydrolysed Metabolites in Bovine Milk by Liquid Chromatography-Tandem Mass Spectrometry. *Chin. J. Anal. Chem.* **2012**, *40*, 757–761.
18. Zheng, Y.; Shi, Z.; Wu, W.; He, C.; Zhang, H. Label-Free DNA Electrochemical Aptasensor for Fumonisin B1 Detection in Maize Based on Graphene and Gold Nanocomposite. *J. Anal. Chem.* **2021**, *76*, 252–257.
19. Ren, W.; Xu, Y.; Huang, Z.; Li, Y.; Tu, Z.; Zou, L.; He, Q.; Fu, J.; Liu, S.; Hammock, B.D. Single-chain variable fragment antibody-based immunochromatographic strip for rapid detection of fumonisin B(1) in maize samples. *Food Chem.* **2020**, *319*, 126546. [[CrossRef](#)]
20. Kinghorn, A.B.; Fraser, L.A.; Liang, S.; Shiu, S.C.-C.; Tanner, J.A. Aptamer Bioinformatics. *Int. J. Mol. Sci.* **2017**, *18*, 2516. [[CrossRef](#)]
21. Zhang, H.; Li, F.; Dever, B.; Li, X.-F.; Le, X.C. DNA-Mediated Homogeneous Binding Assays for Nucleic Acids and Proteins. *Chem. Rev.* **2012**, *113*, 2812–2841. [[CrossRef](#)] [[PubMed](#)]
22. Taghdisi, S.M.; Danesh, N.M.; Nameghi, M.A.; Bahreyni, A.; Ramezani, M.; Alibolandi, M.; Emrani, A.S.; Abnous, K. Co-delivery of doxorubicin and α -PCNA aptamer using AS1411-modified pH-responsive nanoparticles for cancer synergistic therapy. *J. Drug Deliv. Sci. Technol.* **2020**, *58*, 101816. [[CrossRef](#)]
23. Farzin, L.; Sadjadi, S.; Shamsipur, M.; Sheibani, S.; Mousazadeh, M.H. Employing AgNPs doped amidoxime-modified polyacrylonitrile (PAN-oxime) nanofibers for target induced strand displacement-based electrochemical aptasensing of CA125 in ovarian cancer patients. *Mater. Sci. Eng. C Mater. Biol. Appl.* **2019**, *97*, 679–687. [[PubMed](#)]
24. Talari, F.F.; Bozorg, A.; Faridbod, F.; Vossoughi, M. A novel sensitive aptamer-based nanosensor using rGQDs and MWCNTs for rapid detection of diazinon pesticide. *J. Environ. Chem. Eng.* **2020**, *9*, 104878. [[CrossRef](#)]
25. Chen, X.; Huang, Y.; Duan, N.; Wu, S.; Xia, Y.; Ma, X.; Zhu, C.; Jiang, Y.; Ding, Z.; Wang, Z. Selection and characterization of single stranded DNA aptamers recognizing fumonisin B1. *Microchim. Acta* **2014**, *181*, 1317–1324. [[CrossRef](#)]
26. Dong, H.; Gao, W.; Yan, F.; Ji, H.; Ju, H. Fluorescence Resonance Energy Transfer between Quantum Dots and Graphene Oxide for Sensing Biomolecules. *Anal. Chem.* **2010**, *82*, 5511–5517. [[CrossRef](#)]
27. Zha, C.; An, X.; Zhang, J.; Wei, L.; Zhang, Q.; Yang, Q.; Li, F.; Sun, X.; Guo, Y. Indirect signal amplification strategy with a universal probe-based lateral flow immunoassay for the rapid quantitative detection of fumonisin B1. *Anal. Methods* **2021**, *14*, 708–716. [[CrossRef](#)]
28. Qin, Y.; Li, S.; Wang, Y.; Peng, Y.; Han, D.; Zhou, H.; Bai, J.; Ren, S.; Li, S.; Chen, R.; et al. A highly sensitive fluorometric biosensor for Fumonisin B1 detection based on upconversion nanoparticles-graphene oxide and catalytic hairpin assembly. *Anal. Chim. Acta* **2022**, *1207*, 339811. [[CrossRef](#)]
29. Sun, Y.; Xu, J.; Li, W.; Cao, B.; Wang, D.D.; Yang, Y.; Lin, Q.X.; Li, J.L.; Zheng, T.S. Simultaneous Detection of Ochratoxin A and Fumonisin B1 in Cereal Samples Using an Aptamer-Photonic Crystal Encoded Suspension Array. *Anal. Chem.* **2014**, *86*, 11797–11802. [[CrossRef](#)]
30. Er Demirhan, B.; Demirhan, B. Investigation of Twelve Significant Mycotoxin Contamination in Nut-Based Products by the LC-MS/MS. *Method. Metab.* **2022**, *12*, 120.
31. Zhao, X.; Gao, J.; Song, Y.; Zhang, J.; Han, Q. Establishment of an Improved ELONA Method for Detecting Fumonisin B₁ Based on Aptamers and Hemin-CDs Conjugates. *Sensors* **2022**, *22*, 6714. [[CrossRef](#)] [[PubMed](#)]